Energy Proceedings
Vol 29, 2022
ISSN 2004-2965

Study on heat dissipation characteristics of jet impingment on structured surface with non-uniform heat flux#

Wenjing Zhang[1], Peng Qian[1],Zizhen Huang[1], Zhiwei Chen[1], Kai Han[1], Jialei Zhang[1], Chang Liu[1], Minghou Liu[1*]

[1]Department of Thermal Science and Energy Engineering,University of Science and Technology of China, 96 JinZhai Rd. Baohe District, Hefei, 230026, China

*Corresponding Author: mhliu@ustc.edu.cn

ABSTRACT

In order to improve the temperature uniformity and reduce the maximum temperature of the surface with Gaussian heat flux, a radiator with jet impinging on the structured surface was proposed in this paper. The effects of Reynolds number and structured surface geometry were observed. The heat transfer performance for three structured surfaces were compared with smooth wall configuration under the same conditions. As the Reynolds number increases, Nu appears with multiple local peaks in the radial direction, which is attributed to the increase of turbulent kinetic energy and the change of flow field. Among three structured surfaces, the rectangular rib has the best performance both in heat transfer and temperature uniformity, followed by the cubic rib, both of which have strong disturbance to the flow field. Due to larger thermal resistance of heat conduction, the convex structure exhibits worst heat transfer performance.

Keywords: jet impingement heat transfer, Gaussian heat flux, structured surface

NONMENCLATURE

Abbreviations	
D	jet nozzle diameter[mm]
H	jet-plate distance[mm]
D_c	diameter of impacted plate[mm]
u	average jet velocity[m/s]
Re	jet Reynolds number, uD/ν
q	heat flux[w/m^2]
Nu	local Nusselt number
Nu_s	local Nusselt number of smooth plate
$\overline{Nu}$	average Nusselt number
ΔT	temperature difference of the heating surface[K]
ν	kinematic viscosity[m^2/s]

1. INTRODUCTION

With the advancement of semiconductor processing technology, electronic devices continue to develop towards high integration. Semiconductor lasers are widely used in medical and national defense fields due to their large output energy, high peak power (locally up to 1000w/cm^2), and compact device structure, including laser therapy instrument, lidar, laser communication, etc.[1-4]. Under such non-uniform heating conditions for a long time, the thermal stress distribution on the surface of the thermoelectric device is uneven [5]. When the tensile or compressive strength of the material is exceeded, damage will occur and its life will be seriously damaged [6]. Therefore, it is necessary to take effective cooling measures to improve the temperature uniformity and reduce the maximum temperature of the heating surface.

Jet impingement cooling technology can provide high heat exchange efficiency, and the cooling capacity is remarkable, which is suitable for occasions with high requirements for heat dissipation [7]. In gas turbines, for example, it can be used to cool the location of the greatest heat flow in the turbine vanes to extend the life of the blades. In the glass and plastics industry, impingement jets are used to maintain molding temperature and prevent high temperature deformation [8]. Therefore, impinging jets are used in this paper to cool non-uniform heat flux electronic devices. The heat transfer rate during jet impingement is affected by parameters such as Reynolds number, jet-plate distance, stagnation point radial distance, target plate inclination, target plate roughness, jet confinement, inlet geometry, and turbulence intensity at the inlet. Most of the previous studies focused on the single-hole jet impinging on a smooth plate [9]. Yuet al. [10] conducted a numerical simulation study on the transient temperature change of a single-hole impacting high-temperature plate. The results show that with the decrease of jet-plate distance, the heat transfer near the stagnation point is enhanced, while the heat transfer near the outlet boundary is weakened, and therefore, the temperature uniformity is deteriorated. In all cases, the transient heat transfer increases significantly with increasing Reynolds number. Lytle and Webb [11] investigated the heat dissipation capability of the structure when the distance between the nozzle and the target is less than one nozzle diameter. When z/d < 0.25, the turbulence intensity and velocity increased significantly, and two peaks were observed in the Nusselt number, and the outer peak moved radially outward with the increase of Re. Singh et al. [12] compared the heat transfer capacity of three roughness (cubic, cylindrical, concentric) plates at different nozzle spacing through experiments and numerical calculations, and the concentric roughness performed well in terms of fin efficiency and heat transfer effect. Theoretically, there is no significant increase in pressure loss compared to smooth plates. In addition, they investigated the effects of factors such as nozzle distance from the heat exchange surface, jet Reynolds number, and nozzle geometry. In practical applications, rough surfaces are often used to enhance heat transfer [13].

Aiming at the heat dissipation requirements of Gaussian heat sources commonly used in lidar, a radiator with a jet impinging on a structured surface is proposed in this paper. We carried out numerical analysis of its heat dissipation characteristics and flow field, and improved the disadvantage of poor heat transfer in the stagnation zone by changing the type of strengthening surface.

2. GEOMETRIC MODE AND MATHEMATICAL MODEL

2.1 Model description

Figure 1 shows a schematic diagram of the jet cooling system used in this study. It consists of two parallel large plates, the inlet is located on the upper plate, the diameter of the inlet is 20 mm, directly facing the maximum value of the center of the Gaussian heat source, the diameter of the large circular plate is 100 mm, the jet-plate distance is 10 mm, the thickness of both plates is 2 mm. The deionized water impinges on the bottom plate from the inlet, and after sufficient cooling, flows out from the annular outlet. The bottom surface of the impact plate is loaded with a Gaussian distributed heat source. Considering calculation time and cost, symmetry boundary is applied as shown in Fig.2.

Fig. 1 Geometric model

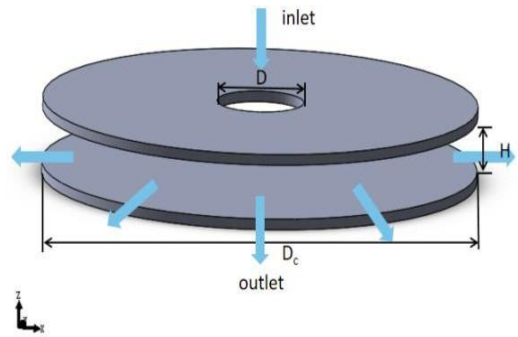

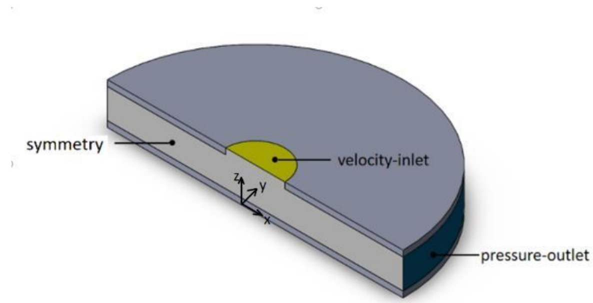

Fig. 2 Boundary conditions

During the continuous heating process of deionized water, its thermophysical parameters will change with temperature. In this study, the thermal conductivity and specific heat capacity of deionized water are considered to change with temperature.

This paper investigates the effect of the following three structured surfaces on heat transfer under non- uniform heat flow:

(1)1 mm square rib

(2)2 mm rectangular rib

(3)1 mm convex surface

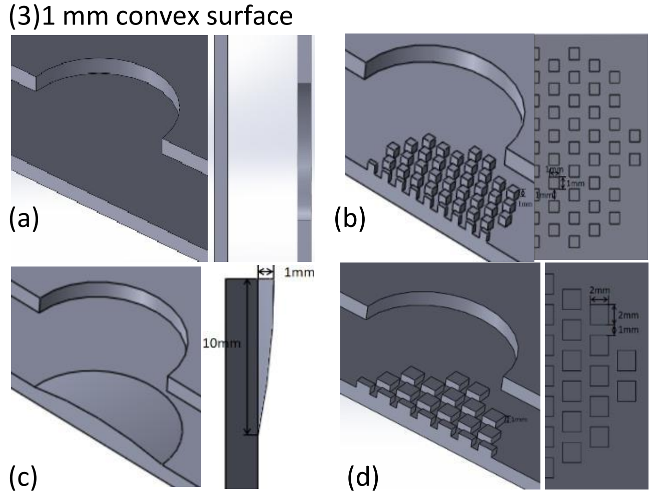

Fig.3 Structural schematic diagram of different modified surfaces (a) smooth plate (b) 1mm square rib (c)2mm rectangular rib (d) 1mm convex surface

2.2 Governing Equations

In order to simplify the analysis, it is assumed that the flow satisfies the steady state incompressibility, and the whole process satisfies the law of conservation of mass, momentum and energy.

The continuous equations for steady state and incompressible flow are:

$$\frac{\partial U_J}{\partial x_j}=0 \tag{1}$$

The momentum conservation equation is:

$$\rho\cdot\frac{\partial\left(U_iU_j\right)}{\partial x_j}=-\frac{\partial p}{\partial x_i}+\frac{\partial}{\partial x_j}\left[\left(\mu+\mu_t\right)\left(\frac{\partial U_i}{\partial x_j}+\frac{\partial U_j}{\partial x_i}\right)\right] \tag{2}$$

The energy conservation equation is:

$$\rho\cdot\frac{\partial\left(U_jc_pT\right)}{\partial x_j}=\frac{\partial}{\partial x_j}\left[\left(\lambda+\frac{c_p\mu_t}{\mathrm{Pr}_t}\right)\frac{\partial T}{\partial x_j}\right] \tag{3}$$

Where ρ is the density, μ is the dynamic viscosity, C_p is the constant pressure specific heat capacity of deionized water, and λ is the thermal conductivity.

2.3 Boundary conditions

Deionized water jet nozzle: the inlet is set as the velocity inlet, and the turbulence intensity of the flow is 5%. The inlet temperature was a constant temperature of 298.15 K. In most jet impingement studies, the impingement Reynolds number is defined as:

$$\mathrm{Re}=\frac{u\cdot D}{\nu} \tag{4}$$

D is the diameter of the inlet impact hole, u is the inlet flow rate, and ν is the kinematic viscosity of the working medium.

(2) Outlet Boundary

In the calculation case, the outlet is set as the pressure outlet boundary condition and the static pressure is 0.

(3) Symmetrical boundary

On the middle symmetry plane, the heat flux is 0.

(4) Heating wall

The Gaussian distribution heat flow boundary condition is given at the bottom of the heat sink, and the heat flux $q=1.7\times10^{6}\cdot exp\left(-975\cdot\left(x^2+y^2\right)^{0.5}\right)$

3. GRID INDEPENDENCE AND TURBULENCE MODEL VALIDATION

3.1 Grid Independence

Mesh independence tests are performed on smooth slabs. Adjust the local size between 0.8 million, 1.56 million, 2.03 million, 2.65 million, and 3.44 million cells. The specific size is shown in the table below.

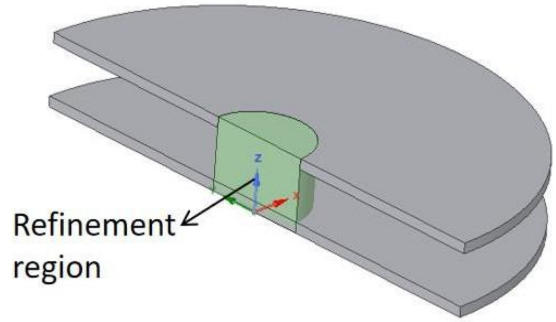

Fig.4 Schematic diagram of refinement region

NO.	Refineds ize	Boundary Layers			Cell Size
		Number of Layers	Growth rate	First Height	
Mesh 1	1.0	4	1.2	0.5	800000
Mesh 2	0.35	4	1.2	0.1	1560000
Mesh 3	0.25	4	1.2	0.02	2030000
Mesh 4	0.2	4	1.2	0.015	2650000
Mesh 5	0.15	5	1.2	0.01	3440000

Tab.1 Grid size

As shown in Fig.5, the temperature accuracy of the heat source loading surface of mesh 1 and mesh 2 is poor, the relative temperature difference between mesh 3 and mesh 4 is 0.9%, and the relative temperature difference between grid 4 and grid 5 is 0.3%. Considering the calculation time and accuracy, a grid model with a grid number of 2.65 million (mesh4) is finally selected for further research.

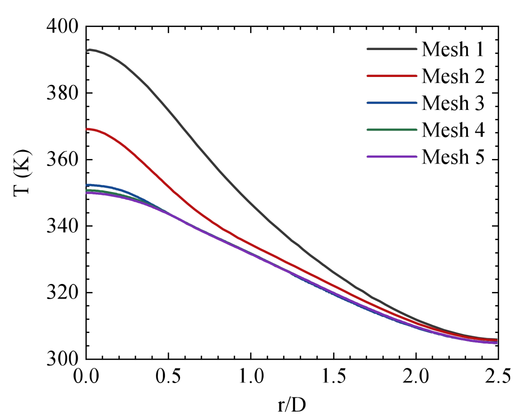

Fig.5 Temperature distribution of heat source loading surface for five grid sizes, H/D = 0.5, Re = 99422

3.2 Model Validation

Zu et al. [14] conducted a numerical simulation of a circular jet impinging vertically on a flat plate and compared it with the existing benchmark experimental data, and found that among seven turbulence models, the Shear Stress Transport (SST k- ω) model and Large Eddy Simulation (LES) models can better predict fluid flow and heat transfer performance with errors of 7% and 4%, respectively, while the remaining models have errors above 30%. The LES computational cost is relatively high, therefore, the SST k- ω model is a good choice after considering the computational accuracy and computational cost.

In order to ensure the accuracy of the simulation results, this paper carried out a numerical simulation of a similar type of circular hole impacting circular plate experiment [15], and also obtained the results of the average Nusselt number variation along the plate, which is compared with the experimental data as shown in Fig.6. The simulation results in this paper are in good agreement with the the experiment, indicating that the grid and turbulence model adopted in this study are feasible.

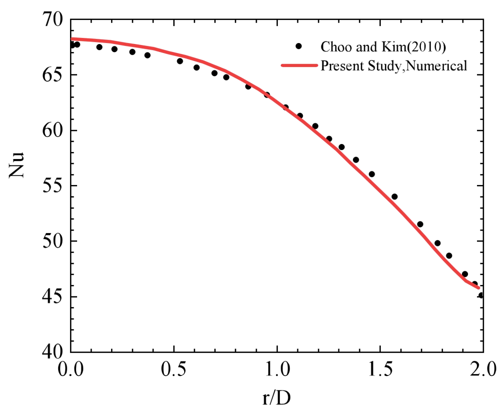

Fig.6 Comparison between present model with the experiment

4. RESULTS AND DISCUSSION

4.1 Influence of Reynolds Number

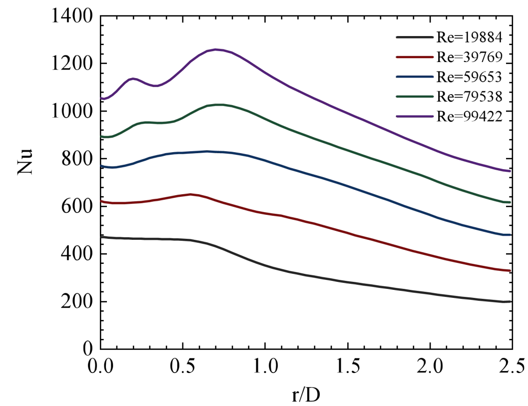

Fig.7 Radial local Nu distribution of smooth plates at different Reynolds numbers

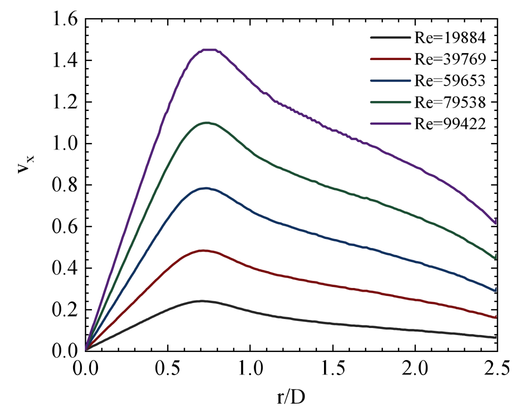

Fig.8 Radial velocity distribution in the near-wall region of a smooth plate under different Reynolds numbers

When the Reynolds number is small, that is, when the fluid inlet velocity is 1 m/s, Nu reaches the maximum value at the stagnation point, and then gradually decreases monotonically in the radial direction. With the increase of Reynolds number, in addition to a maximum value in the stagnation point region, an another local maximum in Nu develops at r/D=0.5-1.0.The reason is that the existence of the pressure gradient in the stagnation zone promotes the fluid to accelerate the flow along the axial direction of the impact target surface. At r/D=0.7, the velocity reaches the maximum value in the radial direction, and the fluid temperature is lower than the downstream, and the momentum exchange is intensified, the turbulence intensity increases, and the heat transfer coefficient increases sharply to form a peak. When Re increases to 79538 and 99422, in addition to the two maxima mentioned above, a third local plateau in Nu develops at r/d = 0.2. The reason may be that with the increase of Re number, the wall jet transitions from free jet to turbulent flow, disturbs the viscous sublayer, thins the thermal boundary layer, increases the local velocity and turbulence intensity to a certain extent, and makes the Nusselt number reach a peak value. Subsequently, in the process of flow, deionized water is continuously heated, and at the same time, affected by the friction of the wall, the flow velocity is reduced, the influence of turbulent flow is weakened, and the heat exchange effect is gradually deteriorated. In the radial direction, the local Nusselt number shows a decreasing trend.

4.2 Influence of structured surface

The comparison of the heat transfer effect between the three structured surfaces and the smooth plate when the Reynolds number is 99422 is studied.

(1) Local Nu

Define the Nusselt number as:

$$Nu = \frac{q_w \cdot D}{(T_w - \frac{T_{in} + T_{out}}{2}) \cdot \lambda} \quad (5)$$

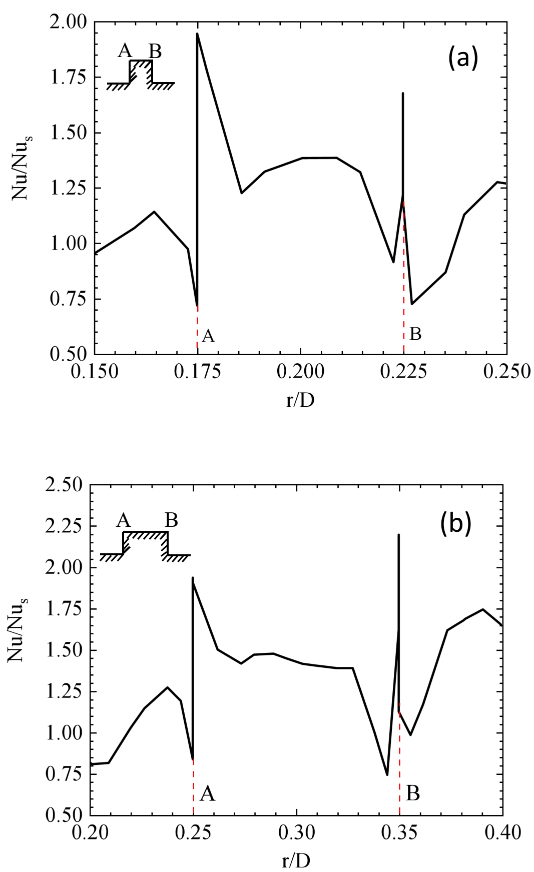

Fig.9 local Nusselt number distributions(a) 1mm square rib (b)2mm rectangular rib

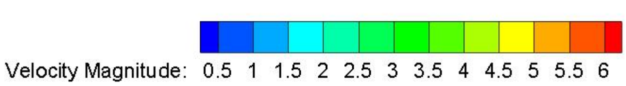

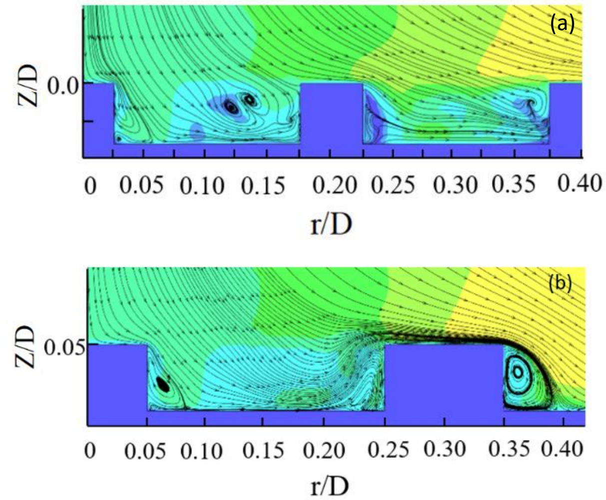

Fig.10 Streamline diagram (a) 1mm square rib (b)2mm rectangular rib

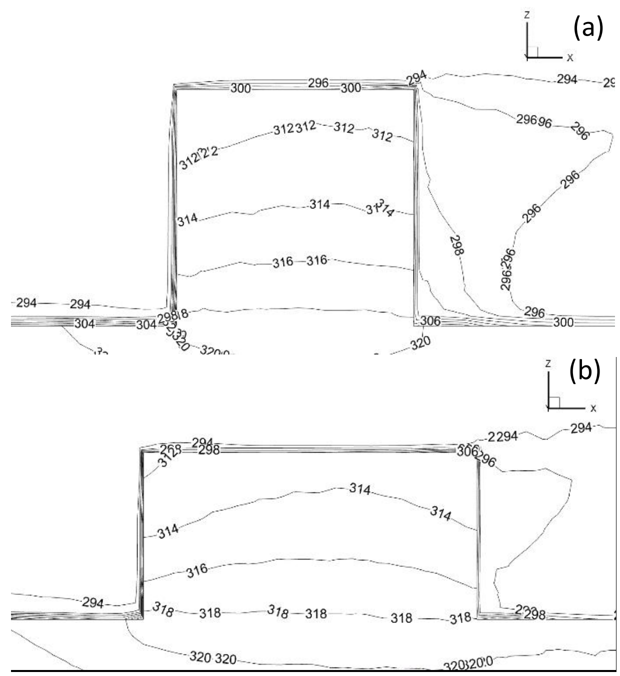

Fig.11 Temperature contours (a) 1mm square rib (b)2mm rectangular rib

Take the rectangular rib as an example , from the Fig.10(b), it can be seen from the streamline diagram that at x/D=0.2, the boundary layer is separated, the fluid disturbance is enhanced, the Nu increases gradually, and a small recirculation zone is generated. Subsequently, the reverse pressure gradient at the front of the square rib separates the boundary layer again, which enhances the turbulence of the flow field. The fluid directly impacts the surface of the rib, which enhances the overall heat transfer. Therefore, the Nusselt number increases quite rapidly along the front surface of the rib. And a maximum is reached near the upstream protruding angle (A) of the flow turn, while the isotherms are tightly packed at A (Fig.9) and the lowest local wall temperature–312K occurs(Fig.11).Then the local Nu gradually decreases until the flow passes the end of the rib top surface, because the thermal boundary layer on the rib top surface becomes thicker. In the area behind the rib, a recirculation zone occurs here, and its temperature is continuously heated to form a local high temperature area. The Nusselt number decreases along the back of the rib until the separation shear layer in the inter-rib reattachment area scours the wall surface,so Nu gradually increases to reach another local maximum in the range of x/D=0.36-0.39. Finally, it tapers off until it encounters the next square rib. Interestingly, the heat transfer at the corners behind the ribs is relatively poor (Nu/Nus< I), but the overall heat transfer is significantly enhanced.

On the two structured surfaces of rectangular rib and cubic rib, the radial distribution trend of Nu is almost the same, but it can be seen from Fig.10 that the low-velocity area and high-temperature area (Fig.11) in the region before and after the rib of the cubic rib are more than those of the rectangular rib. At the same time, due to the large number of cubic ribs, the resistance to fluid flow is large, and the momentum loss increases, so that the maximum lateral velocity that can be achieved in the process of wall jet is smaller than that of rectangular ribs.

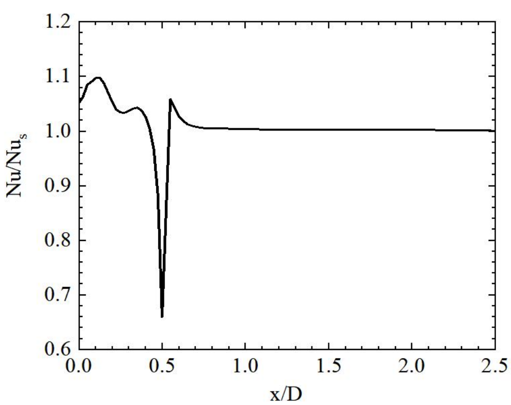

Fig.12 Local Nusselt number distributions of the surface with 1mm convex surface

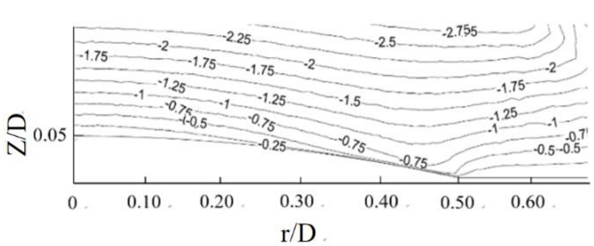

Fig.13 Axial velocity (V_z) contour of the surface with 1mm convex surface

When there is a convex surface structure, the fluid entering the impact hole has an acceleration stage long the x direction, and the surface temperature of the convex structure is also lower than that of the smooth plate, therefore the Nu is slightly larger. However, the heat transfer enhancement is not obvious. With the thickening of the boundary layer, Nu will decrease to a certain extent. As shown in Fig.13, at r/D=0.35, the axial V_z velocity in the near-wall region reaches the maximum value –0.6m/s. At the junction of the convex surface and the flat plate, the axial velocity decreases rapidly, resulting in poor heat transfer at the junction, which is given in Fig.12. After junction point, the fluid is rapidly accelerated along the wall, and Nu increases rapidly.

(2) Average Nu

The above figure shows the change trend of the average Nusselt number. Except for the convex surface which failed to improve the Nusselt number, the cubic and rectangular ribs can improve the average Nusselt number by 4.63% and 5.73%, respectively. The convex surface causesthe Nusselt number to drop by 0.55%. The reason should be that the convex surface does not cause disturbance of the flow field, and the turbulence degree of the flow field hardly changes. On the contrary, increasing of the thickness of the convex surface leads to alarge Bi, and the thermal conduction thermal resistance is much larger than the convection thermal resistance. Thus , it negatively affects heat transfer.

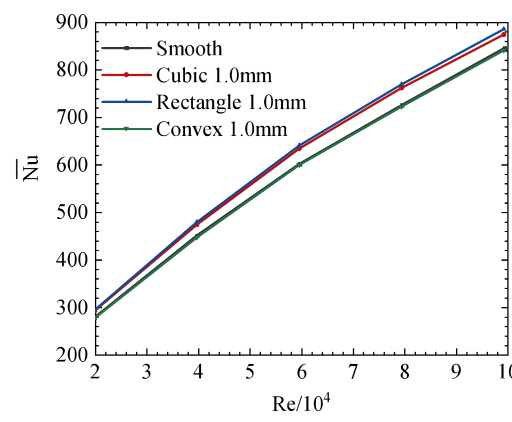

Fig.14 Effect of structured surface on average Nusselt number distributions.

(3) Temperature uniformity

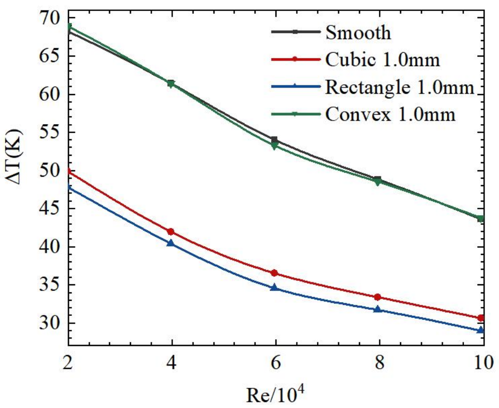

Fig.15 Effect of structured surface on temperature uniformity.

The difference between the highest temperature and the lowest temperature of the heating surface is calculated to characterize the temperature uniformity. Except for the convex surface, the other two rib structures can improve the temperature uniformity, and the larger rectangular rib works better, the temperature difference dropped by almost 20 K compared with smooth wall.

5. CONCLUSION

This paper studied the heat transfer characteristics of a turbulent jet impinging on rough surfaces. The effects of Reynolds number and structured surfaces were observed. The results for the three structured surfaces were compared to smooth surface under the same conditions. As the Reynolds number increases, Nu decreases from monotonic to non-monotonic, and more than one peak appears,the reason is attributed to the increase of turbulence intensity and the change of flow field. Among the three structured surfaces, the rectangular rib has the best heat transfer performance, followed by the cubic rib, both of which have strong disturbance to the flow field, but the convex structure makes the heat transfer effect worse because of larger thermal resistance of heat conduction. Except for the convex surface, the other two rib structures can improve the temperature uniformity.

ACKNOWLEDGEMENT

The authors would like to appreciate the support of the National KeyR&D Program of China [2018YFB1900602] and the National NaturalScience Foundation of China [NSFC Grant No.11372302].

REFERENCE

[1] Chen Tianqi. Research on thermal stress/strain characteristics of high-power semiconductor laser arrays [D]. University of Chinese Academy of Sciences (Xi'an Institute of Optics and Fine Mechanics, Chinese Academy of Sciences), 2018.

[2] Li Zhigang. Research on heat transfer and thermal stress in high-power solid-state lasers [D]. Graduate School of Chinese Academy of Sciences (Institute of Engineering Thermophysics), 2008.

[3] David F W. A brief history of high-power semiconductor lasers. IEEE J. Sel.
Top. Quant., 2000, 6 (6): 1470-1477

[4] Hügel H. New solid-state lasers and their application potentials. Opt. Lasers Eng., 34 (2000) 213-229

[5] Gao Junchao. Theoretical study on the thermal effect of solid-state laser medium. Master's thesis, Huazhong University of Science and Technologystudy, 2004

[6] Hu Hao. Thermal effect and laser characteristics of heat capacity DPL laser medium. Master's thesis, China Institute of Engineering Physics, 2005

[7] K. Jambunathan, etal., A review of heat transfer data for single circular jet
impingement, Int. J. Heat Fluid Flow 13 (1992) 106–115.

[8] Afroz, F. and M.A.R. Sharif, Numerical investigation of heat transfer from a plane surface due to turbulent annular swirling jet impingement. International Journal of Thermal Sciences, 2020. 151.

[9] Sagot, B., et al., Jet impingement heat transfer on a flat plate at a constant wall temperature. International Journal of Thermal Sciences, 2008. 47(12): p. 1610-1619.

[10] Yu, P., et al., Transient heat transfer characteristics of small jet impingement on high-temperature flat plate. International Journal of Heat and Mass Transfer, 2017. 114: p. 981-991.

[11] D. LYTLE and B.W.W., Air jet impingement heat transfer at low nozzle-plate spacings. Inl. J. Heat Mass Transfer., 1994. 31: p. 1687-1697.

[12]Singh, P., et al., *Effect of micro-roughness shapes on jet impingement heat transfer and fin-effectiveness.* International Journal of Heat and Mass Transfer, 2019. 132: p. 80-95

[13] Sriromreun, P. and P. Sriromreun, A Numerical and Experimental Investigation of Dimple Effects on Heat Transfer Enhancement with Impinging Jets. Energies, 2019. 12(5).

[14] Zu, Y.Q.,etal., Numerical Study on Stagnation Point Heat Transfer by Jet Impingement in a Confined Narrow Gap. Journal of Heat Transfer, 2009. 131(9).

[15] Choo, K.S. and S.J. Kim, Comparison of thermal characteristics of confined and unconfined impinging jets. International Journal of Heat and Mass Transfer, 2010. 53(15-16): p. 3366-3371.